



The Discovery of a Luminous $z = 5.80$ Quasar from the Sloan Digital Sky Survey¹

Xiaohui Fan², Richard L. White³, Marc Davis⁴, Robert H. Becker^{5,6}, Michael A. Strauss², Zoltan Haiman², Donald P. Schneider⁷, Michael D. Gregg^{5,6}, James E. Gunn², Gillian R. Knapp², Robert H. Lupton², John E. Anderson, Jr.⁸, Scott F. Anderson⁹, James Annis⁸, Neta A. Bahcall², William N. Boroski⁸, Robert J. Brunner¹⁰, Bing Chen¹¹, Andrew J. Connolly¹², Istvan Csabai¹¹, Mamoru Doi¹³, Masataka Fukugita^{14,15}, G. S. Hennesy¹⁶, Robert B. Hindsley¹⁷, Takashi Ichikawa¹⁸, Željko Ivezić², Avery Meiksin¹⁹, Timothy A. McKay²⁰, Jeffrey A. Munn²¹, Heidi J. Newberg²², Robert Nichol²³, Sadanori Okamura¹³, Jeffrey R. Pier²¹, Maki Sekiguchi¹⁴, Kazuhiro Shimasaku¹³, Alexander S. Szalay¹¹, Gyula P. Szokoly²⁴, Aniruddha R. Thakar¹¹, Michael S. Vogeley²⁵, Donald G. York²⁶

¹Based on observations obtained with the Sloan Digital Sky Survey, which is owned and operated by the Astrophysical Research Consortium, and at the W. M. Keck Observatory, which is operated as a scientific partnership among the California Institute of Technology, the University of California, and NASA, and was made possible by the generous financial support of the W. M. Keck Foundation.

²Princeton University Observatory, Princeton, NJ 08544

³Space Telescope Science Institute, Baltimore, MD 21 218

⁴Department of Astronomy, University of California, Berkeley, CA 94720-3411

⁵Physics Department, University of California, Davis, CA 95616

⁶IGPP/Lawrence Livermore National Laboratory, Livermore, CA 95616

⁷Department of Astronomy and Astrophysics, The Pennsylvania State University, University Park, PA 16802

⁸Fermi National Accelerator Laboratory, P.O. Box 500, Batavia, IL 60510

⁹University of Washington, Department of Astronomy, Box 351580, Seattle, WA 98195

¹⁰ Department of Astronomy, California Institute of Technology, Pasadena, CA 91125

¹¹ Department of Physics and Astronomy, The Johns Hopkins University, 3701 San Martin Drive, Baltimore, MD 21218, USA

¹² Department of Physics and Astronomy, University of Pittsburgh, Pittsburgh, PA 15260

¹³Department of Astronomy and Research Center for the Early Universe, School of Science, University of Tokyo, Hongo, Bunkyo, Tokyo, 113-0033, Japan

¹⁴Institute for Cosmic Ray Research, University of Tokyo, Midori, Tanashi, Tokyo 188-8502, Japan

¹⁵Institute for Advanced Study, Olden Lane, Princeton, NJ 08540

¹⁶U.S. Naval Observatory, 3450 Massachusetts Ave., NW, Washington, DC 20392-5420

¹⁷Remote Sensing Division, Code 7215, Naval Research Laboratory, 4555 Overlook Ave. SW, Washington, DC 20375

¹⁸Astronomical Institute, Tohoku University, Aoba, Sendai 980-8578 Japan

¹⁹ Institute for Astronomy, University of Edinburgh, Edinburgh EH9 3HJ, UK

²⁰University of Michigan, Department of Physics, 500 East University, Ann Arbor, MI 48109

²¹U.S. Naval Observatory, Flagstaff Station, P.O. Box 1149, Flagstaff, AZ 86002-1149

²²Rensselaer Polytechnic Insitute, Dept. of Physics, Applied Physics, and Astronomy, Troy, NY 12180

²³ Department of Physics, Carnegie Mellon University, Pittsburgh, PA 15213

²⁴ Astrophysikalisches Institut Potsdam An der Sternwarte 16 D-14482 Potsdam, Germany

²⁵Department of Physics, Drexel University, 3141 Chestnut St., Philadelphia, PA 19104

ABSTRACT

We present observations of SDSSp J104433.04–012502.2, a luminous quasar at $z = 5.80$ discovered from Sloan Digital Sky Survey (SDSS) multicolor imaging data. This object was selected as an i' -band dropout object, with $i^* = 21.8 \pm 0.2$, $z^* = 19.2 \pm 0.1$. It has an absolute magnitude $M_{1450} = -27.2$ ($H_0 = 50 \text{ km s}^{-1} \text{ Mpc}^{-1}$, $q_0 = 0.5$). The spectrum shows a strong and broad Ly α emission line, strong Ly α forest absorption lines with a mean continuum decrement $D_A = 0.91$, and a Lyman Limit System at $z = 5.72$. The spectrum also shows strong OI and SiIV emission lines similar to those of quasars at $z \lesssim 5$, suggesting that these metals were produced at redshift beyond six. The lack of a Gunn-Peterson trough in the spectrum indicates that the universe is already highly ionized at $z \sim 5.8$. Using a high-resolution spectrum in the Ly α forest region, we place a conservative upper limit of the optical depth due to the Gunn-Peterson effect of $\tau < 0.5$ in regions of minimum absorption. The Ly α forest absorption in this object is much stronger than that in quasars at $z \lesssim 5$. The object is unresolved in a deep image with excellent seeing, implying that it is unlensed. The black hole mass of this quasar is $\sim 3 \times 10^9 M_\odot$ if we assume that it is radiating at the Eddington luminosity and no lensing amplification, implying that it resides in a very massive dark matter halo. The discovery of one quasar at $M_{1450} < -27$ in a survey area of 600 deg^2 is consistent with an extrapolation of the observed luminosity function at lower redshift. The abundance and evolution of such quasars can provide sensitive tests of models of quasar and galaxy formation.

1. Introduction

At what epoch did the first generation of galaxies and quasars form? How was the universe re-ionized, ending the “dark ages” (Rees 1998)? These fundamental questions can only be answered with studies of high-redshift objects. The last few years have witnessed the first direct observations of galaxies at redshift higher than five (Dey et al. 1998, Weymann et al. 1998, Spinrad et al. 1998, Chen, Lanzetta & Pascarelle 1999, van Breugel et al. 1999, Hu et al. 1999, see also the review by Stern & Spinrad 1999), while detailed studies of the ensemble properties and large scale distribution of galaxies at $z \sim 4$ have begun (Steidel et al. 1998, 1999). Several quasars have been found at $z \gtrsim 5$ (Fan et al. 1999, 2000a, Zheng et al. 2000), including a low-luminosity quasar at $z = 5.50$ (Stern et al. 2000).

²⁶University of Chicago, Astronomy & Astrophysics Center, 5640 S. Ellis Ave., Chicago, IL 60637

Studies of high-redshift quasars provide important probes of this critical epoch in cosmic evolution. The lack of the Gunn-Peterson (1965) effect in the absorption spectrum of a $z \sim 5.0$ quasar (Songaila et al. 1999) indicates that the universe is already highly ionized at that redshift. The exact epoch of re-ionization could be determined from the absorption spectra of quasars at even higher redshift (Miralda-Escudé 1997, Haiman & Loeb 1999). The study of the luminosity function of high-redshift quasars will constrain models of quasar and galaxy evolution (Haiman & Loeb 1998, Haehnelt et al. 1999), and determine whether it was UV radiation from AGNs or from young massive stars that re-ionized the universe, ending the “dark ages” (Haiman & Loeb 1998). Measurements of the chemical abundance in the quasar environment will reveal the metal production process at the very early stage of galaxy evolution (Hammann & Ferland 1999). Finally, luminous high-redshift quasars represent high peaks of density fields, and may be the markers of large scale structure at these early epochs (Djorgovski et al. 1999, Haiman & Hui 2000, Martini & Weinberg 2000).

The Sloan Digital Sky Survey (SDSS; York et al. 2000) is using a dedicated 2.5m telescope and a large format CCD camera (Gunn et al. 1998) at the Apache Point Observatory in New Mexico to obtain images in five broad bands (u' , g' , r' , i' and z' , centered at 3540, 4770, 6230, 7630 and 9130 Å, respectively; Fukugita *et al.* 1996) over 10,000 deg² of high Galactic latitude sky. The multicolor data from SDSS have proven to be very effective in selecting high-redshift quasars: more than 50 quasars at $z > 3.5$ have been discovered to date from about 600 deg² of imaging data (Fan et al. 1999, 2000a, Schneider et al. 2000, Zheng et al. 2000). The inclusion of the reddest band, z' , in principle enables the detection of quasars up to $z \sim 6.5$ in SDSS data.

In this paper, we report the discovery of SDSSp J104433.04–012502.2 (the name reflecting its J2000 coordinates from the preliminary SDSS astrometry, accurate to $\sim 0.1''$ in each coordinate), a very luminous, “ i' -dropout” quasar at $z = 5.80$, selected by its very red $i^* - z^*$ color. In a Λ -dominated flat universe ($H_0 = 65 \text{ km s}^{-1} \text{ Mpc}^{-1}$, $\Lambda = 0.65$ and $\Omega = 0.35$, referred to as the Λ -model in this paper, Ostriker & Steinhardt 1995, Krauss & Turner 1995), $z = 5.80$ corresponds to an age of 0.9 Gyr in an universe 13.9 Gyr old, or a look-back time of 93.2% of the age of the universe. Similarly, the universe was 0.7 Gyr old at $z = 5.80$ in a universe 13.0 Gyr old at present for a model with $\Omega = 1$ and $H_0 = 50 \text{ km s}^{-1} \text{ Mpc}^{-1}$, which we refer to as the $\Omega = 1$ model in this paper. We present the photometric observations and target selection in §2, and the spectroscopic observations in §3. In §4, we discuss the cosmological implications, including the constraints on the Gunn-Peterson effect, quasar evolution models, and black hole formation.

2. Photometric Observation and Target Selection

The object SDSSp J104433.04–012502.2 (hereafter SDSS 1044–0125 for brevity) was selected from the SDSS imaging data based on its extremely red $i^* - z^*$ color. The photometry of this object is summarized in Table 1. The photometric observations of this region were obtained by the SDSS imaging camera on 2000 March 4 during the SDSS commissioning phase. For off-equator scans, the telescope moves along a great circle, with the photometric camera drift-scanning at the sidereal rate. The effective exposure time is 54.1 seconds in each band. The seeing in the i' and z' bands was about $1.9''$. The photometric calibration is provided by an auxiliary 20-inch telescope at the same site (Uomoto et al. 2000, in preparation). The photometric zeropoint is accurate to about 7% in u' and z' and 2% in g' , r' and i' . Because the definition of the photometric system is not yet finalized, we quote measured magnitudes using asterisks (e.g., i^*) to represent preliminary photometry, while referring to the filters with primes (e.g., i'). SDSS 1044–0125 is undetected in u' , g' and r' . The object is detected at the $5\text{-}\sigma$ level in the i' band. The z' detection is of very high significance, with $i^* - z^* = 2.58 \pm 0.20$. Data are quoted as asinh magnitudes (Lupton, Gunn & Szalay 1999) and are on the AB magnitude system (Fukugita *et al.* 1996). Finding charts for SDSS 1044–0125 in the i' and z' bands are shown in Figure 1.

As shown by Fan (1999), the colors of high-redshift quasars are strong functions of redshift in the SDSS filter system, as first the Ly α forest and then the Lyman Limit Systems move through the filter system. At $z > 3.6$, quasars become very red in $g^* - r^*$ while remaining blue in $r^* - i^*$, and can be readily distinguished from stars based on these colors. At $z > 4.6$, quasars become very red in $r^* - i^*$. They are easily distinguished from red stars in the $r^* - i^*$ vs. $i^* - z^*$ color-color diagram (Fan et al. 1999, 2000a). Quasars at $z \sim 5.5$ have very similar $r^* - i^*$ and $i^* - z^*$ colors to those of late M stars. Finally, at $z \gtrsim 5.7$, the Ly α emission line begins to move out of the SDSS i' filter. With a predicted $i^* - z^* \gtrsim 2$, quasars at such redshifts become i' -band dropout objects. However, unlike the lower-redshift g' and r' -dropout quasars, these quasars have only one measurable optical color, as they will be completely undetected in r' . The SDSS alone cannot provide a constraint on the quasar’s continuum shape redward of the Ly α emission. It is thus difficult to distinguish them from other classes of red objects without additional information, such as near-infrared photometry (see also Zheng et al. 2000) or detection in the radio or X-ray.

In fact, the only other known class of stellar objects with such red colors ($i^* - z^* \gtrsim 2$) are the extremely cool stars/substellar objects with spectral type L or T (Kirkpatrick et al. 1999, Strauss et al. 1999, Tsvetanov et al. 2000, Fan et al. 2000b, Leggett et al. 2000). Most of these objects are brown dwarfs with mass below the hydrogen burning limit.

Although L and T dwarfs are very rare on the sky (the density for L dwarfs is 1 per $\sim 15 \text{ deg}^2$ for $i^* < 20$, Fan et al. 2000b), they are still more numerous than are $z > 5$ quasars, and are the major contaminants of searches for i' -dropout quasars. Near infrared photometry can be used to separate high-redshift quasar candidates from these cool dwarfs: the continuum shape of quasars is relatively flat towards near-IR bands, while the flux of L dwarfs continues to rise sharply towards longer wavelengths.

We have selected i' -dropout candidates with $i^* - z^* \gtrsim 2$ and $z^* < 19.5$ from about 600 deg^2 of SDSS imaging data. These 600 deg^2 overlap the publicly released area of the Two Micron All Sky Survey (2MASS). SDSS 1044–0125 is the only i' -dropout source in the 2MASS covered area that is *not detected* at the $7\text{-}\sigma$ level in any band in the 2MASS Point Source Catalog. All other sources are detected in at least one band at more than 10σ (e.g. Fan et al. 2000b, Leggett et al. 2000).

Is the non-detection in 2MASS sufficient to rule out the possibility that SDSS 1044–0125 is a brown dwarf? In this area of the sky, the 2MASS Point Source Catalog has $7\text{-}\sigma$ limiting magnitudes of roughly $J = 16.7$, $H = 15.9$ and $K_s = 15.0$. This indicates a $7\text{-}\sigma$ upper limit on the optical-IR colors of SDSS 1044–0125: $z^* - J < 2.5$, $z^* - H < 3.3$ and $z^* - K_s < 4.2$. There are three L dwarfs in Fan et al. (2000b) that have $i^* - z^* > 2$: SDSS 0330–0025 ($i^* - z^* = 2.13$, spectral type L2), SDSS 0539–0059 ($i^* - z^* = 2.31$, L5) and SDSS 1326–0038 ($i^* - z^* = 2.61$, L8). They all have $z^* - J \gtrsim 2.7$, $z^* - H \gtrsim 3.6$ and $z^* - K_s \gtrsim 4.2$ (see Tables 2 and 5 in Fan et al. 2000b). Although the current L dwarf sample is small, the $i^* - z^*$ and the $z^* - J$ (or H , K_s) colors seem to be reasonable indicators of the spectral type for L dwarfs (Kirkpatrick et al. 1999, Fan et al. 2000b). Therefore, if SDSS 1044–0125 ($i^* - z^* = 2.6$) had been an L dwarf, we would expect it to have been detected by 2MASS with high significance. Thus the non-detection in the 2MASS passbands indicates that SDSS 1044–0125 is unlikely to be a L dwarf, but is rather a source with a much flatter IR continuum, such as a quasar at $z > 5.6$ or a compact galaxy at $z > 1$.

A K' -band image of SDSS 1044-0125 was obtained on the night of 2000 April 17, using the Near Infrared Camera (NIRC, Matthews & Soifer 1994) on the Keck I telescope under photometric skies and good seeing. The observations consisted of a nine-point dither pattern, integrating for $3 \times 10\text{s}$ coadds at each location. The data were flattened, sky-subtracted, shifted, and stacked using the DIMSUM package in IRAF. The images show SDSS 1044-0125 to be an unresolved point source with $\text{FWHM} = 0''.375$. Photometry through a $2''$ radius aperture yields $K' = 17.02 \pm 0.04$, referenced to the standards of Persson et al. (1998). There are no companions or associated structure within $20''$ of the quasar to a 3σ point source limiting magnitude of $K' \approx 22.3$.

3. Spectroscopy

Low and high dispersion spectra of SDSS 1044–0125 were obtained with the Echelle Spectrograph and Imager (ESI; Epps & Miller 1998) on the Keck II telescope on the night of 2000 April 6. The night was photometric with 0.9'' seeing. A 1200 second exposure was taken through a 0.7'' slit in the low-dispersion mode of ESI. In this mode, a prism is used for dispersion. The spectrum covers 3900 Å to about 10000 Å. The dispersion varies roughly linearly with wavelength from 0.8 Å/pixel at 3900 Å to 10 Å/pixel at 10000 Å. In addition, two 1200 second high resolution spectra were taken through a 1.0'' slit in the echellette mode of ESI. In this mode, the spectral range of 3900 Å to 11000 Å is covered in ten spectral orders with a constant dispersion of 11.4 km s⁻¹ pixel⁻¹. Wavelength calibrations were performed with observations of Hg-Ne-Xe lamps in the low-dispersion prism mode, and a Cu-Ar lamp in the echellette mode. The spectrophotometric standard G191-B2B (Massey 1988, Massey & Gronwall 1990) was observed for flux calibration. All observations were carried out at the parallactic angle. The data were reduced with standard IRAF routines.

Figure 2 shows the final spectrum combining the low and high dispersion observations (total exposure time of 3600s), over a wavelength range of 4500 - 10000 Å, and binned to 4 Å/pixel. The telluric absorption bands were removed using the standard star spectrum. The absolute flux scale of the spectrum is adjusted so that it reproduces the SDSS z^* magnitude. The signal-to-noise ratio at $\lambda > 8000$ Å is 15 – 20 per pixel. The spectrum of SDSS 1044–0125 shows the unambiguous signature of a very high redshift quasar: the broad and strong Ly α +NV emission line at $\lambda \sim 8300$ Å with a sharp discontinuity to the blue side, due to the onset of very strong Ly α forest absorption. The flux level drops by a factor of ~ 10 from the red side to the blue side of the Ly α +NV emission. A Ly β +OVI emission line is detected at ~ 7000 Å, with an additional flux decrement due to the onset of Ly β forest absorption lines. The spectrum shows no detectable flux at $\lambda < 6100$ Å because of the presence of a Lyman Limit System (see §4). Redward of Ly α , two additional emission lines, OI+SiIII λ 1302 and SiIV+OIV] λ 1400 are also clearly visible. The synthetic $i^* - z^*$ color calculated from the spectrum in Figure 2 is 2.5, consistent with the SDSS measurement.

The redshift determination of such an object is not straightforward. The Ly α emission line is severely affected by the strong Ly α forest lines (as well as by possible internal absorption lines). For $z \sim 4$ quasars, Schneider, Schmidt & Gunn (1991) show that the peak of the Ly α emission line is typically at rest-frame 1219 Å, but with a large scatter. Another strong line, CIV λ 1549, is out of the range of our spectrum. OI+SiIII λ 1302 and SiIV+OIV] λ 1400 are relatively weak. We use the central wavelengths of these two blends from Francis et al. (1991). Gaussian fits of these two lines are listed in Table 2. Based on

these fits, we adopt a redshift of 5.80 ± 0.02 for SDSS 1044–0125. Objective measurement of the equivalent width of the Ly α line is difficult (see the discussion by Schneider, Schmidt & Gunn 1991). Using the continuum level determined from the red side of Ly α emission, we find the rest-frame equivalent width of Ly α + NV is $\sim 26 \text{ \AA}$. However, this number is clearly an underestimate due to the extreme Ly α absorption, maybe by a factor of two. Figure 2 indicates that the expected line center of Ly α at $z = 5.80$ is severely absorbed, and that the blue wing of the line has almost completely disappeared. The measurement of the Ly β +OVI line is difficult as well. We smooth the spectrum of Figure 2 to estimate the continuum level, and find an equivalent width of $\sim 30 \text{ \AA}$. This value is also highly uncertain due to the difficulty in defining a “continuum” in the Ly α forest region.

It is interesting to note that the strengths of the OI+SiII λ 1302 and SiIV+OIV] λ 1400 line blends are comparable to those at much lower redshift: the average rest frame equivalent widths of these two lines are $3.2 \pm 0.4 \text{ \AA}$ and $8.1 \pm 0.6 \text{ \AA}$ in the sample of 30 quasars at $z \sim 4$ in Schneider, Schmidt & Gunn (1991), compared to 3.4 and 7.0 \AA in the case of SDSS 1044–0125. Previous studies have shown that quasar environments at $z \sim 4$ have roughly solar or higher metallicities (Hammann & Ferland 1999). Although we cannot derive the metallicity of SDSS 1044–0125 based on these emission line measurements, the existence of strong lines suggests that in this system, the metallicity is already quite high at this redshift. Assuming the metals were produced in stellar evolution, the initial starburst and chemical enrichment of the quasar environment must have happened at a very early epoch.

From the spectrum in Figure 2, we derive its continuum AB magnitude at rest frame 1280 \AA , $AB_{1280} = 19.28$, after correcting for interstellar extinction ($E(B - V) = 0.054$, from the map of Schlegel, Finkbeiner & Davis 1998). In the Λ -model (see §1), SDSS 1044–0125 has an absolute magnitude $M_{1280} = -27.41$. Assuming a power law continuum with $f_\nu \propto \nu^{-0.5}$ we find $M_{1450} = -27.50$ and $M_B = -27.96$. In the $\Omega = 1$ model (§1) it has $M_{1280} = -27.15$, $M_{1450} = -27.24$, and $M_B = -27.70$. In this cosmology, the nearby luminous quasar 3C273 has $M_B = -27.0$. SDSS 1044–0125 is a very luminous quasar, about twice as luminous as 3C 273 (assuming that it is not amplified by lensing or beaming).

SDSS 1044–0125 is detected neither in the FIRST radio survey (Becker, White & Helfand 1995) at the 1mJy level at 20cm wavelength, nor in the ROSAT All Sky Survey (Voges et al. 1999), implying a 3- σ upper limit of $3 \times 10^{-13} \text{ ergs cm}^{-2} \text{ s}^{-1}$ in the 0.1 – 2.4 keV band. These result is not unexpected; only a few $z > 4$ quasars have observed X-ray or radio fluxes above this value (Kaspi, Brandt & Schneider 2000, Schmidt et al. 1995). A deep exposure with Chandra or XMM is needed to determine its X-ray properties.

4. Discussion

4.1. Absorption Properties and Gunn-Peterson Effect

The high luminosity of SDSS 1044–0125 makes it an ideal object for high signal-to-noise ratio observations to study the intergalactic medium at high redshift. In order to detect continuum break caused by the Lyman Limit System, an edge filter with width of 40 Å was convolved with the low resolution spectrum in Figure 2. A strong peak at 6131 Å is detected in the convolved spectrum, indicating the existence of a Lyman Limit System at $z_{LLS} = 5.72$. No flux is detected blueward of this break. A Lyman Limit System is usually detected within 0.1 of the emission redshift in essentially all quasars at $z > 4$ (Schneider, Schmidt & Gunn 1991, Storrie-Lombardi et al. 1996, Fan et al. 1999).

The most striking feature of the spectrum of SDSS 1044–0125 is the very strong absorption caused by Ly α forest lines. However, the flux level in the Ly α forest region never reaches zero. It lacks the Gunn-Peterson (1965) trough that would exist in the spectrum of a quasar at redshift higher than the re-ionization redshift (Haiman & Loeb 1999), indicating that the intergalactic medium is already highly ionized at $z \sim 5.8$. We estimate the average continuum decrements as: $D_{A,B} \equiv \langle 1 - f_{\nu}^{obs}/f_{\nu}^{con} \rangle$, where f_{ν}^{obs} and f_{ν}^{con} are the observed and the unabsorbed continuum fluxes of the quasar, and D_A and D_B measure the decrements in the region between rest-frame Ly α and Ly β ($\lambda = 1050 - 1170$ Å) and between Ly β and the Lyman Limit ($\lambda = 920 - 1050$ Å), respectively (Oke & Korycansky 1982). The measurements of D_A and D_B require knowledge of the continuum shape redward of Ly α . However, with D_A approaching unity, the effect of different slopes is quite small. Assuming a power law continuum ν^{α} with $\alpha = -0.5$, as indicated in Figure 3, we obtain $D_A = 0.91$ and $D_B = 0.94$. Using a slope of -1.0 only changes the D_A and D_B values to 0.92 and 0.96, respectively. We therefore adopt $D_A = 0.91 \pm 0.02$ and $D_B = 0.95 \pm 0.02$. These values are in close accordance with those from quasar RD J030117+002025 ($z = 5.50$, Stern et al. 2000) and from distant galaxies in the Hubble Deep Field (Weymann et al. 1998), and are much higher than that of the $z = 5.00$ quasar SDSSp J033829.31+002156.3 ($D_A = 0.75$, Songaila et al. 1999), suggesting that the strong evolution of the strength of the Ly α forest at $z > 5$, $N(z) \propto (1+z)^{2.3-2.75}$, measured at redshifts below five continues to a redshift of nearly six. Assuming this number density evolution, Zuo (1993) and Fan (1999) show that at $z \sim 5.8$, the expected average D_A ranges from 0.8 to 0.9.

We further derive an upper limit on the Gunn-Peterson optical depth following Songaila et al. (1999). Figure 3 shows the high-resolution echellette spectrum of SDSS 1044–0125 in the Ly α forest region (binned to 2 Å/pixel). The continuum level is approximated by a $\nu^{-0.5}$ power law as above. Even the most transparent part of the forest does not return close

to the continuum level at this resolution. It is evident that the Ly α forest is much stronger in SDSS 1044–0125 than in SDSSp J033829.31+002156.3 (Figure 2 of Songaila et al. 1999), where a fraction of the forest has flux comparable to the extrapolated continuum. In the region between 7926 Å and 7929 Å, SDSS 1044–0125 has an optical depth $\tau = 0.35 \pm 0.07$, where the error bar only reflects the statistical noise in the spectrum (note the noise level indicated in the figure). This value changes to 0.40 and 0.31 for power law slopes of 0.0 and -1.0 , respectively. Therefore, we adopt a conservative limit of $\tau < 0.5$ at this redshift of 5.52. With higher resolution and signal-to-noise ratio, we might be able to select regions even less affected by the Ly α forest lines. Therefore, it is only an upper limit. For comparison, Songaila et al. derived $\tau < 0.1$ for $z = 4.72$ with similar resolution.

The Gunn-Peterson effect analysis above is based on an attempt to measure the amount of flux between Ly α forest lines (e.g., Giallongo et al. 1994). At redshift higher than five, even with a moderately high resolution spectrum, these forest lines overlap, making it impossible to find a truly “line-free” region. Modern hydrodynamic simulations and semi-analytic models show that under the influence of gravity, the intergalactic medium becomes clumpy, and the Gunn-Peterson optical depth should vary even in the lowest column density regions (e.g. Bi, Börner & Chu 1992, Miralda-Escudé & Rees 1993, Cen et al. 1993, Hernquist et al. 1996). The minimum absorption regions in the forest merely represent regions that are most underdense in this fluctuating Gunn-Peterson effect. An accurate measurement of the Gunn-Peterson effect and the ionizing background from the high resolution spectrum of SDSS 1044–0125 requires detailed comparison with cosmological simulations; this is beyond the scope of the current paper.

Figure 2 also shows the detection of an intervening MgII absorption system. The MgII doublet $\lambda 2796.4 + 2803.5$ is detected at wavelengths 9166.7 Å and 9190.3 Å in the high-resolution spectrum; the redshift of this system is $z_{abs} = 2.278$. The rest frame equivalent widths of the doublet lines are 2.43 and 1.90 Å, respectively. This system is very similar to the one detected in SDSSp J033829.31+002156.3 ($z_{abs} = 2.304$, Songaila et al. 1999). It is possible that SDSS 1044–0125 is amplified by lensing from this intervening absorber. However, we saw in § 2 that this object is *unresolved* under 0.4'' seeing in the K band.

4.2. Number Density of Very High Redshift Quasars

The total area of SDSS imaging data that we have searched for high-redshift quasars thus far is of order 600 deg². All that satisfy $z^* < 19.3$ and $i^* - z^* > 2.2$ in this 600 deg² region have been observed spectroscopically. Only SDSS 1044–0125 is identified as

a high-redshift quasar; the remaining objects are L and T dwarfs. Using the luminosity function and redshift dependence of Schmidt, Schneider & Gunn (1995) (for the $\Omega = 1$ model), extrapolating it to higher redshifts and assuming $f_\nu \propto \nu^{-0.5}$, we predict that in a total area of 600 deg², for $z > 5.65$ (i' -dropout objects), there should be 1.5 quasars with $M_{1450} < -27.0$ and 1.1 quasars with $M_{1450} < -27.2$. For $z > 5.8$, the extrapolation predicts 1.1 and 0.8 quasars for $M_{1450} < -27.0$ and -27.2 , respectively. This assumes that our selection efficiency is 100%. The Schmidt-Schneider-Gunn luminosity function is derived using objects with $2.7 < z < 4.7$ and $-27.5 < M_B < -25.5$. Although it is difficult to draw any reliable conclusion from the observation of a single high-redshift quasar, the discovery of SDSS 1044-0025 is consistent with the expectations from this rather large extrapolation from lower redshift results. Assuming that the same luminosity function holds at even higher redshift, the SDSS will be able to discover one quasar at $z \gtrsim 6$, $z^* \lesssim 19$ in every 1500 deg² of the survey.

SDSS 1044-0125 is a very luminous quasar. Assuming that (1) its bolometric luminosity equals the Eddington luminosity, $L_{\text{bol}} = L_{\text{Edd}} = 1.5 \times 10^{38} (M_{\text{BH}}/M_\odot)$ erg s⁻¹; (2) its intrinsic continuum spectrum is the same as the mean spectral template of Elvis et al. (1994), and (3) neither beaming nor lensing affects the observed flux, we find a black hole mass of $M_{\text{BH}} = 3.4 \times 10^9 M_\odot$ in the Λ -model, or $M_{\text{BH}} = 2.7 \times 10^9 M_\odot$ in the $\Omega = 1$ model. In either case, the implied black hole mass is quite large, similar to that of the black hole at the center of the nearby giant elliptical galaxy M87 (Harms et al. 1994, Macchetto et al. 1997). If the quasar were radiating below the Eddington limit, the inferred black hole mass would be even higher. In the Elvis et al. (1994) template, $\approx 1\%$ of the bolometric luminosity is emitted in the observed z' band. If this fraction is larger for SDSS 1044-0125, the implied black hole mass would be reduced. Note that the universe was less than 1 Gyr old at this redshift, while the Eddington time scale, the e -folding time for the growing of a black hole shining at the Eddington luminosity, is $4 \times 10^7 (\epsilon/0.1)$ yr, where ϵ is the radiative efficiency for the accretion. If the black hole started accreting with an initial mass of $\sim 10^3 M_\odot$ with 10% efficiency, the seed black hole would have to form and begin accreting at redshift well beyond 10 in order to grow to $3 \times 10^9 M_\odot$ at $z = 5.80$ (see also Turner 1991). Forming such a massive black hole in such a short time is a remarkable feat. The observations of high-redshift quasars can be used to constrain the formation epoch of the first star clusters and the fueling process of early black holes.

How likely is it to find a quasar like SDSS 1044-0125 in popular cold dark matter cosmological models? We use the following simple model to estimate the abundance of high-redshift quasars (see also Haiman & Hui 2000): Magorrian et al. (1998) have found a correlation between central black hole mass and bulge mass, $M_{\text{BH}}/M_{\text{bulge}} = 6 \times 10^{-3}$ in nearby galaxies. If this correlation holds at high redshift, this would imply a bulge mass of

$5.7 \times 10^{11} M_{\odot}$ (Λ -model) or $4.5 \times 10^{11} M_{\odot}$ ($\Omega = 1$) for the host galaxy of SDSS 1044-0125, and a lower limit of $5.7 \times 10^{12} M_{\odot}$ (Λ -model) or $4.5 \times 10^{12} M_{\odot}$ ($\Omega = 1$) for its dark halo, assuming $M_{\text{halo}}/M_{\text{bulge}} \geq \Omega_{\text{DM}}/\Omega_{\text{b}} \approx 10$.

The comoving abundance of dark matter halos at this epoch is very sensitive to this halo mass, and can be estimated by means of the Press & Schechter (1974) formalism. In a Λ -CDM model, assuming $\sigma_8 = 0.87$ and an untilted primordial power spectrum, for parent halo masses of $10^{12} M_{\odot}$, $6 \times 10^{12} M_{\odot}$, and $10^{13} M_{\odot}$, we expect 50,000, 60, and 4 candidate halos respectively within the survey volume in a redshift window $\Delta z = 1$. The duty cycle of quasar activity is poorly known, but is certainly much less than unity (Haiman & Hui 2000). Given these uncertainties, this model is not contradictory to our discovery of a single quasar like SDSS 1044-0125 in the 600 deg² survey area.

Note that this model does not address the physical process by which the massive black hole formed. The assumptions we made about $M_{\text{BH}}/M_{\text{bulge}}$ and the lifetime of the quasars are completely untested at high redshift. Indeed, Rix et al. (1999) argue that the host galaxies of $z \sim 2$ quasars are appreciably less luminous than the universal $M_{\text{BH}}/M_{\text{bulge}}$ hypothesis would imply. Because of its high luminosity, SDSS 1044-0125 likely probes the exponential, high-mass tail of the underlying dark halo distribution, making predictions of the expected number counts also sensitive to cosmological parameters, especially the normalization of the power spectrum (i.e. σ_8). In principle, the SDSS survey will be able to probe quasars ≈ 1 mag fainter than SDSS 1044-0125, and could reveal tens of additional sources at $z \approx 6$. The detection of these objects will yield strong constraints on cosmological models for the formation and evolution of quasars at very high redshifts.

The Sloan Digital Sky Survey (SDSS) is a joint project of the University of Chicago, Fermilab, the Institute for Advanced Study, the Japan Participation Group, The Johns Hopkins University, the Max-Planck-Institute for Astronomy, Princeton University, the United States Naval Observatory, and the University of Washington. Apache Point Observatory, site of the SDSS, is operated by the Astrophysical Research Consortium. Funding for the project has been provided by the Alfred P. Sloan Foundation, the SDSS member institutions, the National Aeronautics and Space Administration, the National Science Foundation, the U.S. Department of Energy, and Monbusho, Japan. The SDSS Web site is <http://www.sdss.org/>. This publication makes use of data products from the Two Micron All Sky Survey, which is a joint project of the University of Massachusetts and the Infrared Processing and Analysis Center/California Institute of Technology, funded by NASA and NSF. XF and MAS acknowledge additional support from Research Corporation, NSF grant AST96-16901, the Princeton University Research Board, and a Porter O. Jacobus Fellowship. RHB acknowledges support from the Institute of Geophysics and

Planetary Physics (operated under the auspices of the U.S. Department of Energy by the University of California Lawrence Livermore National Laboratory under contract No. W-7405-Eng-48). ZH acknowledges support from Hubble Fellowship grant HF-01119.01-99A. DPS acknowledges support from NSF grant AST99-00703. We thank Wolfgang Voges, Hans-Walter Rix, David Weinberg, and Peng Oh for helpful comments, and the expert assistance of Bob Goodrich and Terry McDonald during the Keck observations.

REFERENCES

- Becker, R. H., White, R. L., & Helfand, D. J. 1995, *ApJ*, 450, 559
- Bi, H., Börner, G., & Chu, Y. 1992, *A&A*, 266, 1
- Cen, R., Miralda-Escudé, J., Ostriker, J. P., & Rauch, M. 1994, *ApJ*, 437, L9
- Chen, H.-W., Lanzeta, K. M., & Pascarella, S. 1999, *Nature*, 398, 586
- Dey, A., Spinrad, H., Stern, D., Graham, J. R., & Chaffee, F. 1998, *ApJ*, 498, L93
- Djorgovski, S. G., Odewahn, S. C., Gal, R. R., Brunner, R., de Carvalho, R. R. 1999, *astro-ph/9908142*
- Elvis, M., Wilkes, B. J., McDowell, J. C., Green, R. F., Bechtold, J., Willner, S. P., Oey, M. S., Polowski, E., & Cutri, R. 1994, *ApJS*, 95, 1
- Epps, H.W., & Miller, J.S. 1998, *Proc. SPIE*, 3355, 48
- Fan, X. 1999, *AJ*, 117, 2528
- Fan, X. et al. 1999, *AJ*, 118, 1
- , 2000a, *AJ*, 119, 1
- , 2000b, *AJ*, 119, 928
- Francis, P.J., Hewett, P.C., Foltz, C.B., Chaffee, F.H., Weymann, R.J., & Morris, S.L. 1991, *ApJ*, 373, 465
- Fukugita, M., Ichikawa, T., Gunn, J.E., Doi, M., Shimasaku, K., & Schneider, D.P. 1996, *AJ*, 111, 1748
- Giallongo, E., D’Odorico, S., Fontana, A., McMahon, R. G., Savaglio, S., Cristiani, S., Molaro, P., & Trevese, D. 1994, *ApJ*, 425, L1

- Gunn, J. E., & Peterson, B. A. 1965, ApJ, 142, 1633
- Gunn, J.E., et al. 1998, AJ, 116, 3040
- Haehnelt, M. G., Natarajan, P., & Rees, M. J. 1998, MNRAS, 300, 817
- Haiman, Z., & Hui, L. 2000, ApJ, submitted (astro-ph/0002190)
- Haiman, Z., & Loeb, A. 1998, ApJ, 503, 505
- , 1999, ApJ, 519, 479
- Hamann, F. & Ferland, G. 1999, ARA&A, 37, 487
- Harms, R.J. et al. 1994, ApJ, 435, L35
- Hernquist, L., Katz, N., Weinberg, D. H., & Miralda-Escudé, J. 1996, ApJ, 457, L51
- Hu, E. M., McMahon, R. G., & Cowie, L. L. 1999, ApJ, 522, L9
- Kaspi, S., Brandt, W. N., & Schneider, D. P. 2000, AJ, in press (astro-ph/0001299)
- Kirkpatrick, J. D., et al. 1999, ApJ, 519, 802
- Krauss, L., & Turner, M. 1995, Gen. Rel. Grav., 27,1137
- Leggett, S. K., et al. 2000, ApJL, in press (astro-ph/0004408)
- Lupton, R.H., Gunn, J.E., & Szalay, A. 1999, AJ, 118, 1406
- Macchetto, F., Marconi, A., Axon, D. J., Capetti, A., Sparks, W., & Crane, P. 1997, ApJ, 489, 579
- Magorrian, J., et al. 1998, AJ, 115, 2285
- Martini, P., & Weinberg, D. H. 2000, ApJ, submitted (astro-ph/0002384)
- Massey, P. 1988, ApJ, 328, 315
- Massey, P., & Cronwall, C. 1990, ApJ, 358, 344
- Matthews, K., & Soifer, B. T. 1994 in *Infrared Astronomy with Arrays*, ed. I. McLean, (Dorchecht: Kluwer), 239
- Miralda-Escudé, J. 1997, ApJ, 501, 15
- Miralda-Escudé, J., & Rees, M. J. 1993, MNRAS, 260, 617

- Oke J.B., & Korycansky D.G. 1982, ApJ, 255, 11
- Ostriker, J. P., & Steinhardt, P. 1995, Nature, 377, 600
- Persson, S. E., Murphy, D. C., Krzeminiski, W., Roth, M., & Rieke, M. J. 1998, AJ, 116, 2475.
- Press, W. H., & Schechter, P. L. 1974, ApJ, 181, 425
- Rees, M. 1999, in *After the Dark Ages: When Galaxies were Young (the Universe at $2 < z < 5$)*, ed. S. S. Holt and E. P. Smith, (AIP Press), 13
- Rix, H.W., Falco, E., Impey, C., Kochanek, C., Lehar, J., McLeod, B., Muñoz, J., & Peng, C. 1999, preprint (astro-ph/9910190)
- Schlegel, D.J, Finkbeiner, D.P., & Davis, M. 1998, ApJ, 500, 525
- Schmidt, M., Schneider D.P., & Gunn, J.E. 1995, AJ, 110, 6
- Schmidt, M., van Gorkom, J.H., Schneider, D.P., & Gunn, J.E. 1995, AJ, 109, 473
- Schneider, D.P, Schmidt, M., & Gunn, J.E. 1991, AJ, 101, 2004
- Schneider, D. P., et al. 2000a, PASP, 112, 6
- Songaila, A., Hu, E. M., Cowie, L., L., & McMahon, R. G. 1999, ApJ, 525, L5
- Spinrad, H., Stern, D., Bunker, A.J., Dey, A., Lanzetta, K., Yahil, A., Pascarelle, S., & Fernández-Soto, A. 1998, AJ, 116, 2617
- Steidel, C.C., Adelberger, K.L., Dickinson, M., Giavalisco, M., Pettini, M., & Kellogg, M.A. 1998, ApJ, 492, 428
- Steidel, C.C., Adelberger, K.L., Giavalisco, M., Dickinson, M., Pettini, M. 1999, ApJ, 519, 1
- Stern, D., & Spinrad, H. 1999, PASP, 111, 1475
- Stern, D., Spinrad, H., Eisenhardt, P., Bunker, A. J., Dawson, S., Stanford, S., & Elston, R. 2000, ApJ, 533, L75
- Storrie-Lombardi, L.J., McMahon, R. G., Irwin, M.J., & Hazard, C. 1996, ApJ, 468, 121
- Strauss, M. A., et al. 1999, ApJ, 522, L61
- Tsvetanov, Z. I., et al. 2000, ApJ, 531, L61

Turner, E. L. 1991, *AJ*, 101, 5

Voges, W., et al. 1999, *A&A*, 349, 389

van Breugel, W., De Breuck, C., Stanford, S. A., Stern, D., Röttgering, H., & Miley, C. 1999, *ApJ*, 518, L61

Weymann, R.J., Stern, D., Bunker, A., Spinrad, H., Chaffee, F.H., Thompson, R.I., & Storrie-Lombardi, L.J. 1998, *ApJ*, 505, L95

York, D. G., et al. 2000, *AJ*, submitted

Zheng, W., et al. 2000, *AJ*, submitted (astro-ph/0005247)

Zuo, L. 1993, *A&A*, 278, 343

Table 1. SDSS and K-band Photometry of SDSSp J10:44:33.04 –01:25:02.2

u^*	g^*	r^*	i^*	z^*	K
22.91	23.91	25.13	21.81	19.23	17.02
± 0.53	± 0.49	± 0.62	± 0.19	± 0.07	± 0.04

The SDSS photometry (u^*, g^*, r^*, i^*, z^*) is reported in terms of *asinh magnitudes* on the AB system. The asinh magnitude system is defined in Lupton, Gunn & Szalay (1999); it becomes a linear scale in flux when the absolute value of the signal-to-noise ratio is less than about 5. In this system, zero flux corresponds to 24.24, 24.91, 24.53, 23.89, and 22.47, in u^* , g^* , r^* , i^* , and z^* , respectively; larger magnitudes refer to negative flux values. The K band photometry is on the Vega-based system. $E(B - V)$ in this direction is 0.054, from Schlegel et al. 1998

Table 2. Emission Line Properties

Line	λ (Å)	redshift	EW (Å, rest frame)
OI+SiII 1302	8858.5 ± 3.8	5.802 ± 0.003	3.4 ± 0.5
SiIV+OIV] 1400	9507.3 ± 3.7	5.789 ± 0.003	7.0 ± 0.4

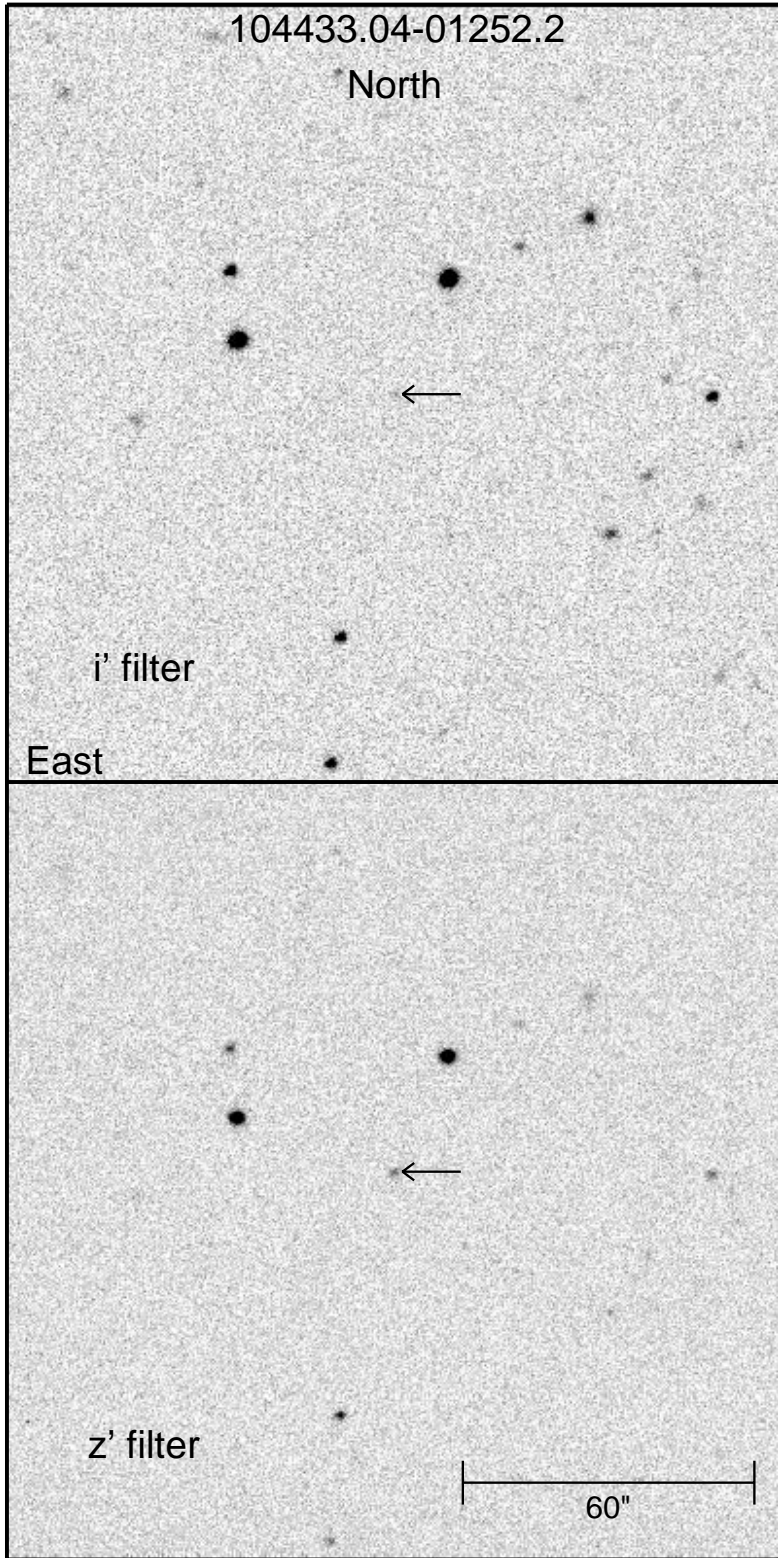


Figure 1. Finding chart for SDSS 1044-0125 (discovery image from the SDSS). The field is 160" on a side. The field is given in both the i' and z' bands (54.1s exposure time).

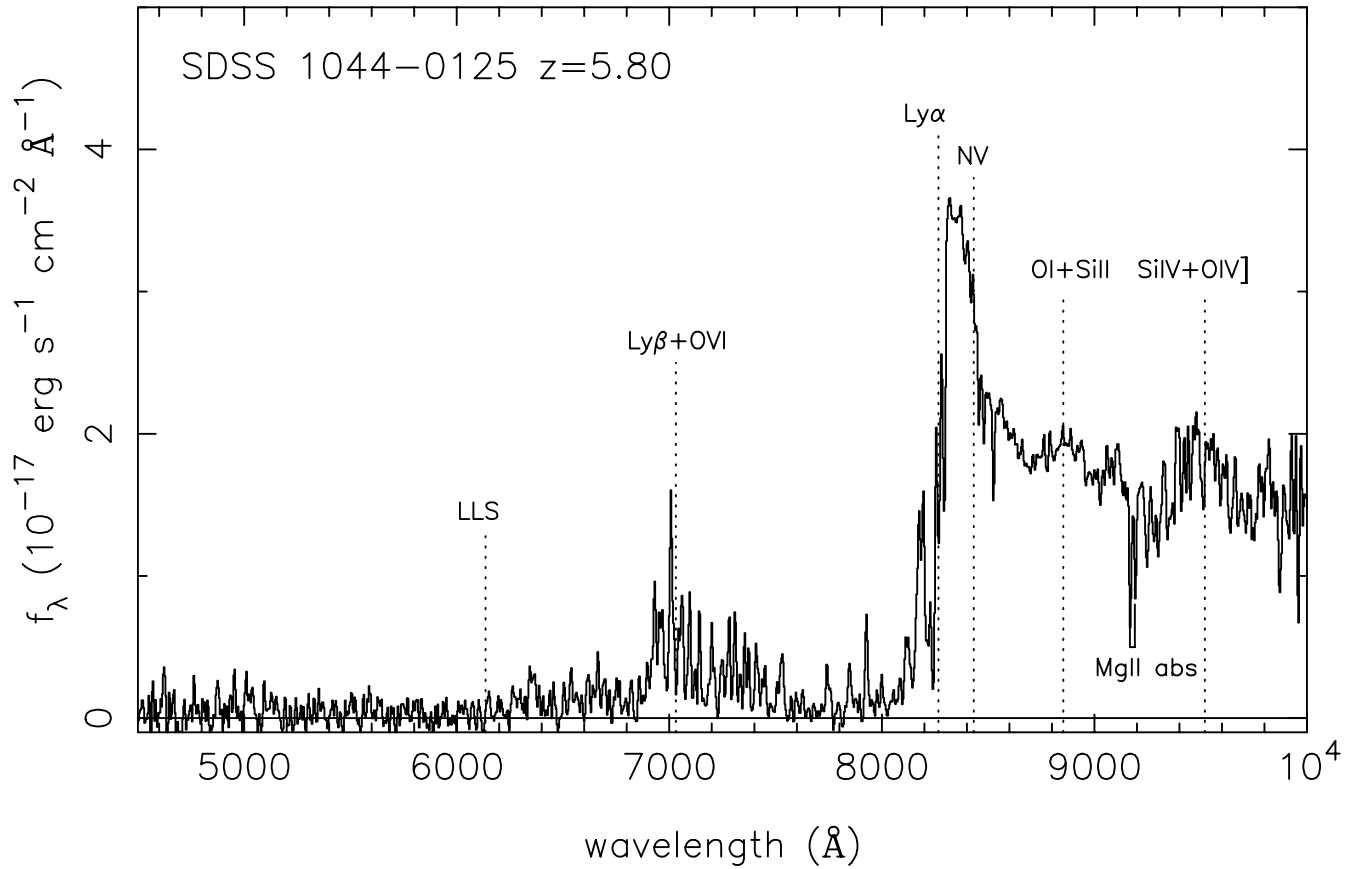


Figure 2. Optical spectrum of SDSS 1044-0125 observed with KeckII/ESI. The total exposure time is 3600s. The spectrum is smoothed to 4 Å/pixel. The spectral resolution is ~ 8 Å at $\lambda = 9000$ Å.

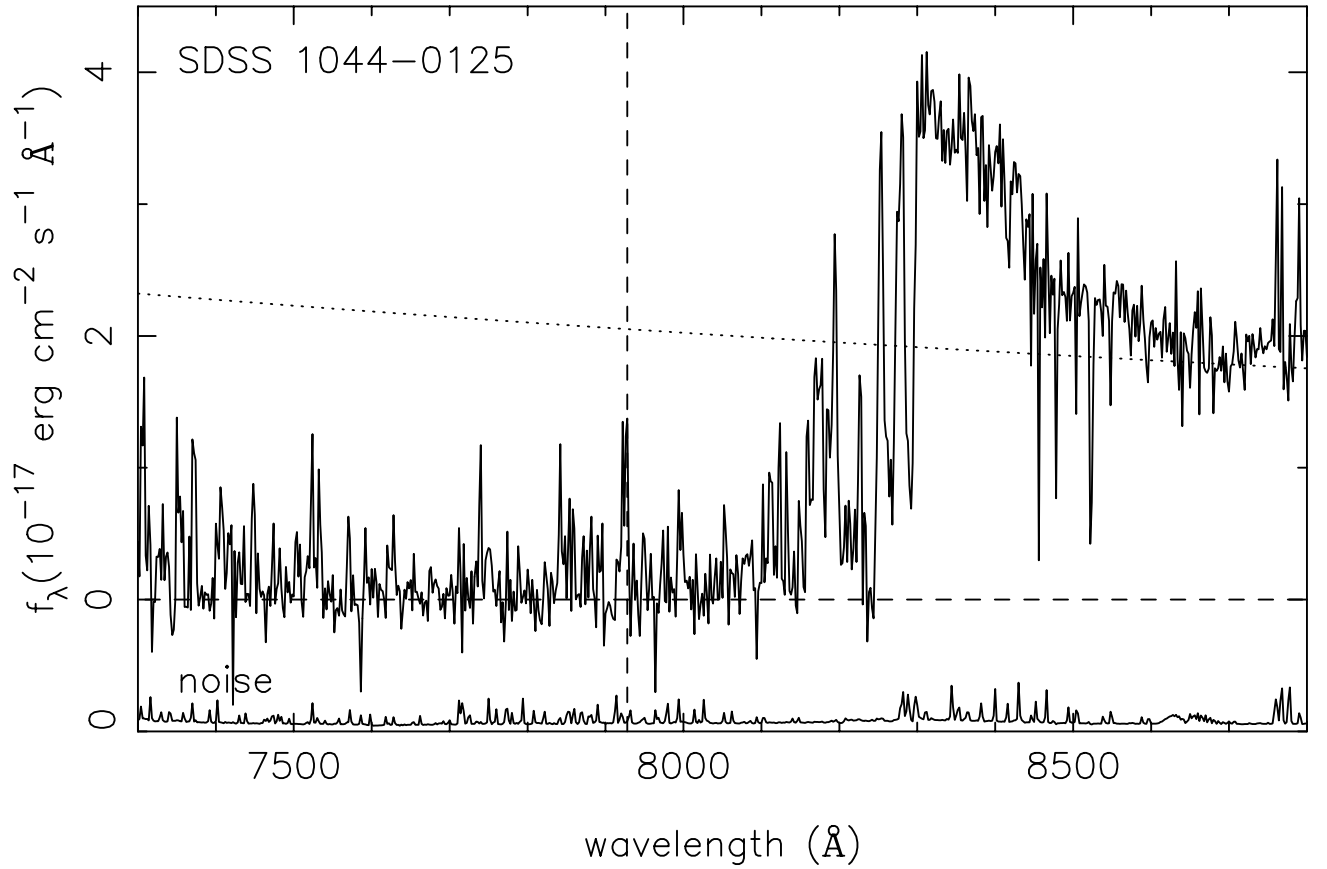


Figure 3. ESI Echelle spectrum over the range 7300 – 8800 \AA . The spectrum has been smoothed to a resolution of 2 \AA . The dotted line shows a $f_\nu \propto \nu^{-0.5}$ continuum, normalized to the region 8650 – 8730 \AA . The dashed line indicates the region with minimum absorption ($\tau \sim 0.4$, see §3.1). The lower panel shows the noise level.